

Self-assembly of double decker cages induced by coordination of perylene bisimide with a trimeric Zn porphyrin: study of the electron transfer dynamics between the two photoactive components

Ana I. Oliva,^a Barbara Ventura,^b Frank Würthner,^c Amaya Camara-Campos,^d Christopher A. Hunter,^d Pablo Ballester,^{*a} and Lucia Flamigni^{*b}

^a Institute of Chemical Research of Catalonia (ICIQ), Avda. Països Catalans 16, 43007 Tarragona, Spain and Catalan Institution for Research and Advanced Studies (ICREA), Passeig Lluís Companys, 23, 08018, Barcelona, Spain. E-mail: pballester@iciq.es

^b Istituto per la Sintesi Organica e la Fotoreattivita (ISOF), Consiglio Nazionale delle Ricerche (CNR) Via P. Gobetti 101, 40129 Bologna, Italy. E-mail: flamigni@isof.cnr.it

^c Institut für Organische Chemie, Universität Würzburg, 97074 Würzburg, Germany.

^d Department of Chemistry, University of Sheffield, Sheffield S3 7HF, United Kingdom.

Supporting Information

- **Titration performed with the model system ZnTPPP and 2 for the calculation of the K_m value for the interaction of the pyridyl nitrogen of 2 to the Zn of ZnTPPP in DCM and TL**
- **$^1\text{H-NMR}$ chemical shift data of the titration of 2 with ZnTTP in DCM**
- **Calculated spectra for the three colored species in equilibrium in DCM/TL titrations**
- **Simulated speciation profiles for the titration of 1b at 1×10^{-5} M in TL**
- **Cyclic voltammogram of ZnTPPP and 2 in DCM**
- **Photophysical properties of 1a and 1b in DCM and TL**
- **Thermodynamic and spectroscopic characterization of model complex 1b₂.3₃ in DCM**
- **Absorption spectra of 1b and the model ZnTPPP in DCM**
- **Emission spectra of models 1b, 2, and 1b₂.3₃ in DCM and TL solutions**

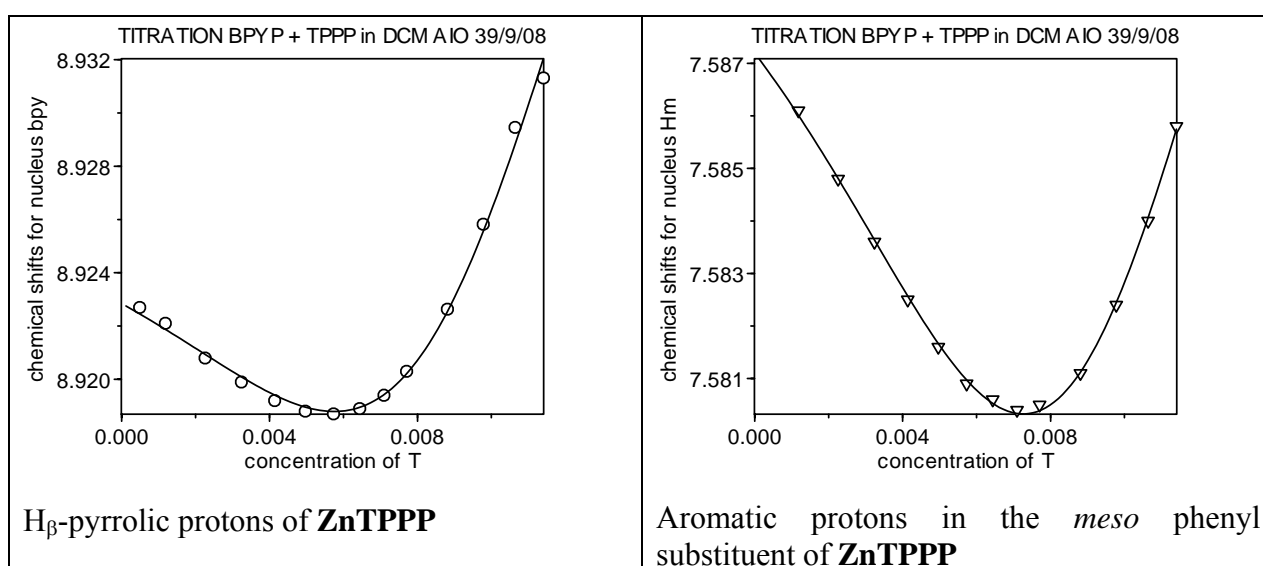
Titration performed with the model system **ZnTPPP** and **2** for the calculation of the K_m value for the interaction of the pyridyl nitrogen of **2** to the Zn of **ZnTPPP**

Dichloromethane. Before examining the interaction of trisporphyrin **1a** with bispyridine perylene **2**, we investigated the properties of a simple model system which cannot assemble into higher order aggregates. This was done in order to characterize the relevant binding interactions for the complexation of bispyridine perylene bisimide **2** with Zn-porphyrins. The coordination of **ZnTPPP** with **2** was first investigated by UV-visible titration in dichloromethane (DCM). Under these dilute conditions (porphyrin concentration $\approx 10^{-5}$ M) we did not observe any significant change in the Soret band of **ZnTPPP**. The bathochromic shift of the Soret band of Zn-porphyrins constitutes the hallmark of axial coordination of nitrogen containing ligands. This result indicates that the stability constants for the axial interaction between the pyridyl-N of **2** and the Zn metal found in the core of **ZnTPPP** is much lower than 10^5 M^{-1} . Consequently, we decided to study the complexation of **ZnTPPP** with **2** using $^1\text{H-NMR}$ spectroscopy ($[\mathbf{2}] = 5 \times 10^{-3} \text{ M}$). The addition of incremental amounts of **ZnTPPP** (stock solution $[\mathbf{ZnTPPP}] = 2.5 \times 10^{-3} \text{ M}$) to a $\text{DCM-}d_2$ solution of **2** induced monotonic and strong upfield changes in the chemical shift values of the signals assigned to the pyridyl protons of **2** ($\Delta\delta(\text{H}_a) = -6.41 \text{ ppm}$ and $\Delta\delta(\text{H}_b) = -1.87 \text{ ppm}$) and more moderate changes also to the upfield region for the signal corresponding to the aromatic proton of the bispyridine perylene core ($\Delta\delta(\text{H}_c) = -0.489 \text{ ppm}$) (See Figure 1 of the manuscript for proton assignments and Table 1S for the complexation induced shifts). These observations suggest that, at this concentration regime, **2** coordinates to **ZnTPPP** units and that the pyridyl residues sitting on the face of the porphyrin experience a large ring-current induced shift. On the other hand, the signals assigned to the β -pyrrolic protons (H_β) and to the aromatic protons of the *meso* phenyl substituents of **ZnTPPP** displayed biphasic behaviour. Thus, during the initial additions of **ZnTPPP** to the $\text{DCM-}d_2$ solution of **2** these protons signals moved upfield, however, when slightly more than one equivalent of **ZnTPPP** was added to the solution the induced chemical shift change was reversed. This type of biphasic behaviour can be assigned to the formation in solution of complexes with different stoichiometry. Due to the ditopic character of the ligand **2**, one could expect that in over a suitable range of concentrations the axial coordination of **ZnTPPP** to bispyridine perylene **2** should lead to the formation of 1:1 and 2:1 complexes. We used the HypNMR2006 software to simultaneously fit all sets of titration data to a binding model assuming free **2**, free **ZnTPPP** and the formation of 1:2 and 1:1 complexes of **2** with **ZnTPPP**. We obtained an excellent fit of the titration data to the theoretical binding curves and a set of reasonable values for the predicted induced chemical shifts values of the protons in the two stoichiometric complexes.

We calculated the following stability constants values $K_{11} = 4 \times 10^3 \text{ M}^{-1}$ and $K_{21} = 4 \times 10^6 \text{ M}^{-2}$ for the **ZnTPPP·2** and **(ZnTPPP)₂·2** complexes respectively. From these calculated values we deduced the microscopic value for the interaction of the pyridyl nitrogen of **2** to the Zn of **ZnTPPP** as $K_m = 2 \times 10^3 \text{ M}^{-1}$ and a cooperativity factor value of $\alpha = 1$ for the coordination of two units of **ZnTPPP** to **2**. Taken together, these results suggest that both binding sites of **2** are independent and the affinity of the pyridyl nitrogen towards **ZnTPPP** is slightly reduced compared to other pyridine derivatives.

Toluene. The binding interactions were also studied using ¹H-NMR spectroscopy in toluene. For titrations of **ZnTPPP** with **2**, we observed an analogous behaviour to that described above for DCM. The β-pyrrolic protons and the aromatic protons of the *meso* phenyl substituents of **ZnTPPP** showed biphasic behaviour while the pyridyl protons and the aromatic protons of the perylene core of **2** moved monotonically upfield. We fit the titration data to a theoretical binding isotherm assuming the formation of two coordination complexes between **ZnTPPP** and **2** with 1:1 and 2:1 stoichiometry. However, due to the low solubility of **2**, the fit obtained for the experimental data to the theoretical binding isotherms was less good than in DCM. Nevertheless, the calculated values for the stability constants of the two complexes, **ZnTPPP · 2** and **(ZnTPPP)₂·2**, are of the same order of magnitude to the ones obtained in dichloromethane solution. From these results we derived a value for the microscopic stability constant for interaction of the pyridyl nitrogen of **2** to the Zn of **ZnTPPP** ($K_m \approx 2 \times 10^3 \text{ M}^{-1}$) in toluene similar to the one calculated in DCM and also a cooperativity factor value of $\alpha \approx 1$ for **2** binding **ZnTPPP** in toluene.

¹H-NMR chemical shift data of the titration of **2** with ZnTTP in DCM



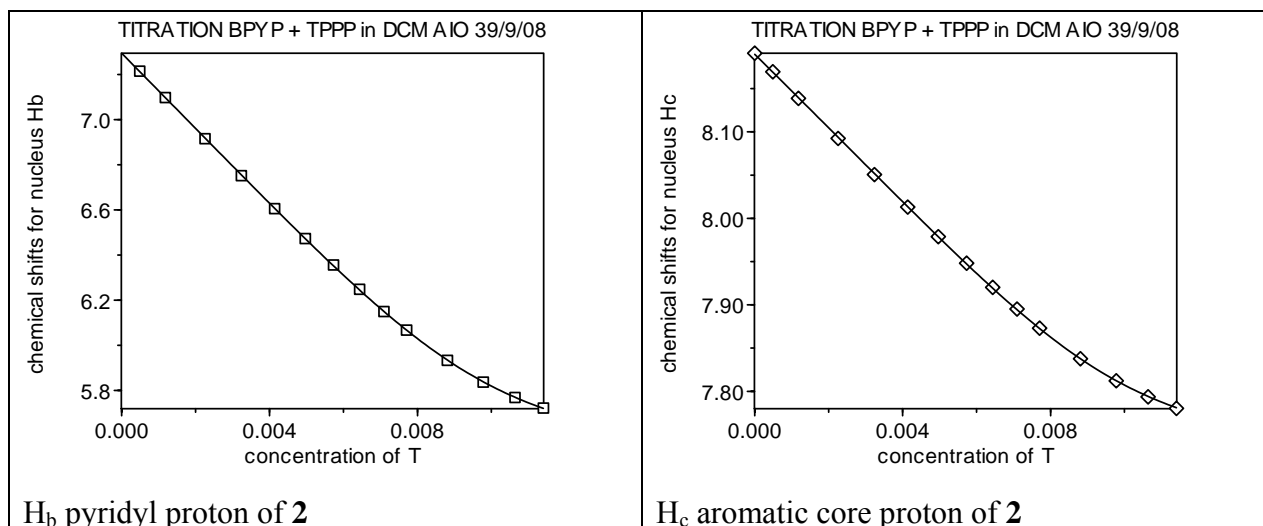


Figure 1S. Experimental chemical shift data (circles, triangles, squares and diamonds) obtained in the ¹H-NMR titration of **ZnTPPP** with **2** in dichloromethane solution. The lines represent the theoretical curves fitted to the experimental points assuming a binding model that considers the formation of two stoichiometric complexes: **ZnTPPP**·**2** (1:1) and (**ZnTPPP**)₂·**2** (2:1).

Table 1S. Calculated chemical shifts values for the different species in the fitting procedure.

species	Proton signals ^a			
	H _β	H _b	H _c	H _{meso}
ZnTPPP	9.02231	-	-	7.63794
2	-	7.29443	8.18975	-
ZnTPPP · 2	8.91977	6.43587	7.97142	7.58563
(ZnTPPP) ₂ · 2	8.89839	5.42755	7.70325	7.56502

^a See Figure 1 in the manuscript for assignment.

Calculated spectra for the three colored species in equilibrium in DCM/TL titrations

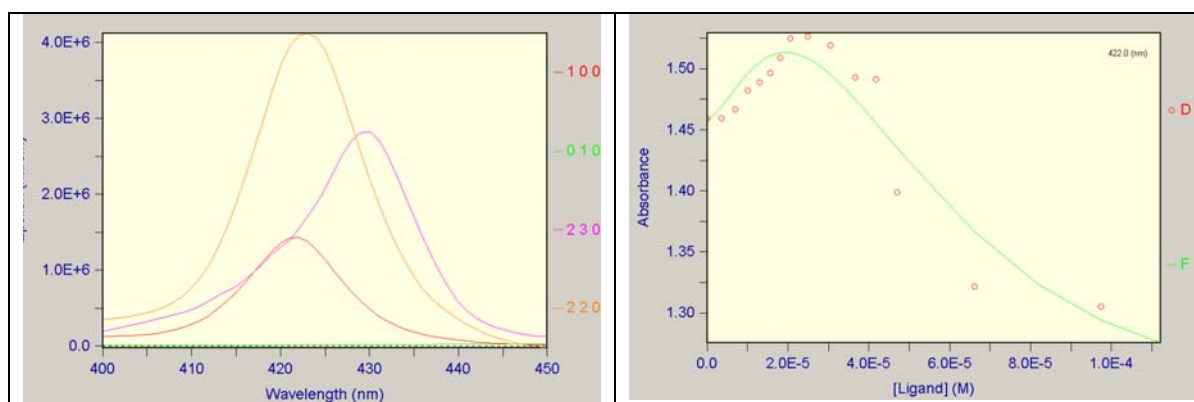


Figure 2S. a) Calculated UV-vis spectra for the three colored species in equilibrium in the DCM titration. b) UV-vis titration data (422 nm) for the binding of **1b** with **2** fitted to the calculated binding curve of a binding model considering free **1b**, **1b**₂·**2** complex and **1b**₂·**2**₃ complex.

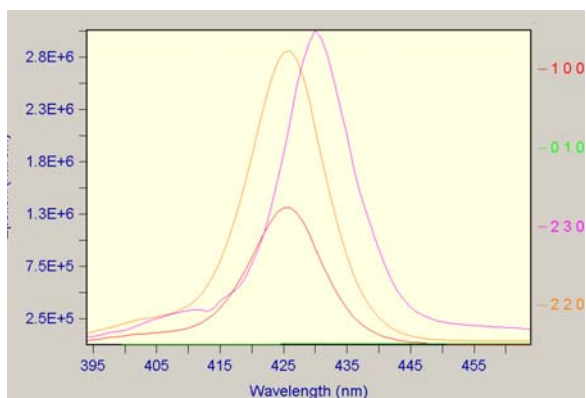


Figure 3S. Calculated UV-vis spectra for the three colored species in equilibrium in the TL titration.

Simulated speciation profiles for the titration of **1b** at 1×10^{-5} M in TL

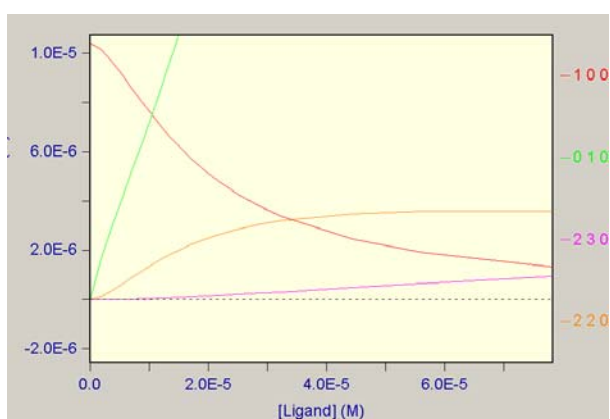


Figure 4S. Simulated speciation profiles for the titration of the Zn-trisporphyrin **1b** at 1×10^{-5} M constant concentration with bispyridine perylene **2** in TL.

Cyclic voltammogram of ZnTPPP and **2** in DCM

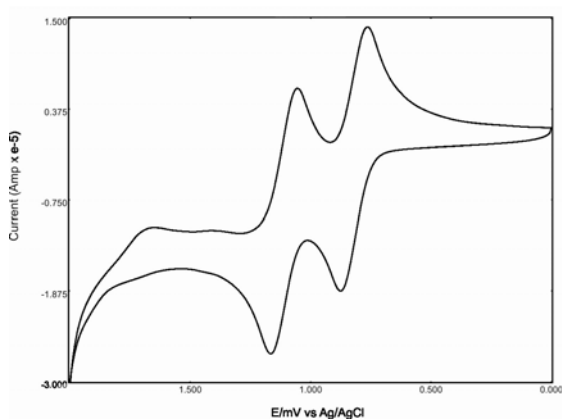


Figure 5S. Cyclic voltammogram of **ZnTPPP** in DCM; scan rate 100 mVs^{-1} . Working electrode: glassy carbon disk; auxiliary electrode: Pt wire; reference electrode: Ag/AgCl; concentration **ZnTPPP** = 1.0 mM; supporting electrolyte: TBA·PF₆ (0.1 M).

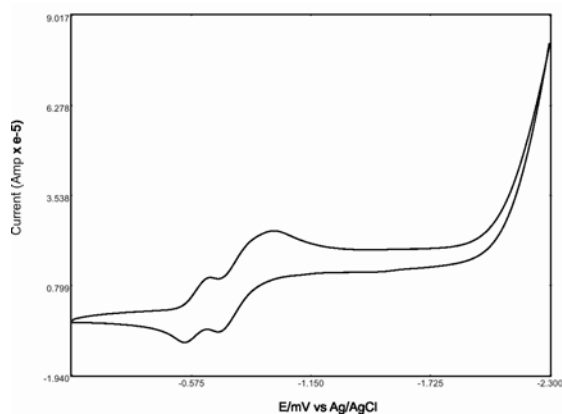


Figure 6S. Cyclic voltammogram of bispyridineperylene **2** in DCM; scan rate 100 mVs^{-1} . Working electrode: glassy carbon disk; auxiliary electrode: Pt wire; reference electrode: Ag/AgCl; concentration [**2**] = 1.0 mM; supporting electrolyte: TBA·PF₆ (0.1 M).

Photophysical properties of **1a** and **1b** in DCM and TL

Absorption spectra of **1a** in toluene and dichloromethane are compared in Figure 7S with the absorption spectra of **1b** in the same solvents. The spectra of the two trisporphyrins in toluene are almost identical, apart from a very modest red-shift (3 nm) of the Soret band of **1a** compared to **1b**. In dichloromethane more pronounced differences appear, in particular a 5 nm red-shift is accompanied by a 30% decrease of the Soret band in **1a** with respect to **1b**. The luminescence spectra are displayed in Figure 8S and the properties are summarized in Table 2S.

Table 2S. Luminescence properties and energy levels of the excited states of **1a** and **1b** in TL and DCM.

		295 K			77 K		
	State	$\lambda_{\max} / \text{nm}$	ϕ_{fl}^c	τ / ns^d	$\lambda_{\max} / \text{nm}$	τ / ns^d	E / eV^e
1a ^a	¹ 1a	602, 648	0.050	1.4	614, 667	2.0	2.02
	³ 1a				799		1.55
1b ^a	¹ 1b	596, 645	0.051	1.9	606, 661	2.2	2.04
	³ 1b				793		1.56
1a ^b	¹ 1a	600, 648	0.038	1.3	617, 671	2.0	2.01
	³ 1a				-		-
1b ^b	¹ 1b	596, 644	0.040	1.6	610, 665	2.4	2.03
	³ 1b				-		-

^aData in toluene. ^bData in dichloromethane. ^cFluorescence quantum yields, the standard used is TPP (tetraphenyl-porphyrin) in aerated toluene ($\Phi_{\text{fl}} = 0.11$). Excitation at 550 nm. ^dExcitation at 560 nm. ^eDerived from the emission maxima at 77 K.

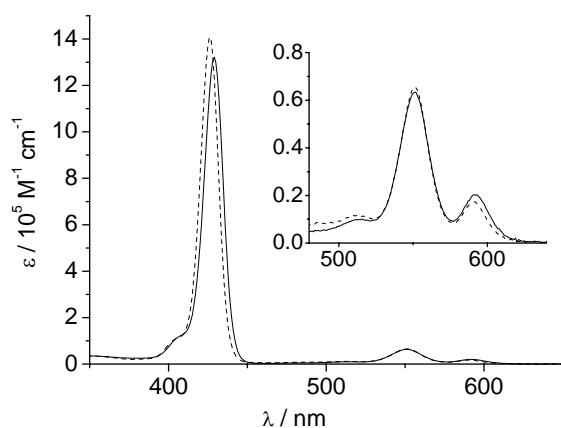


Figure 7S. Absorption spectra of **1a** (solid) and **1b** (dash) in toluene (left) and dichloromethane (right).

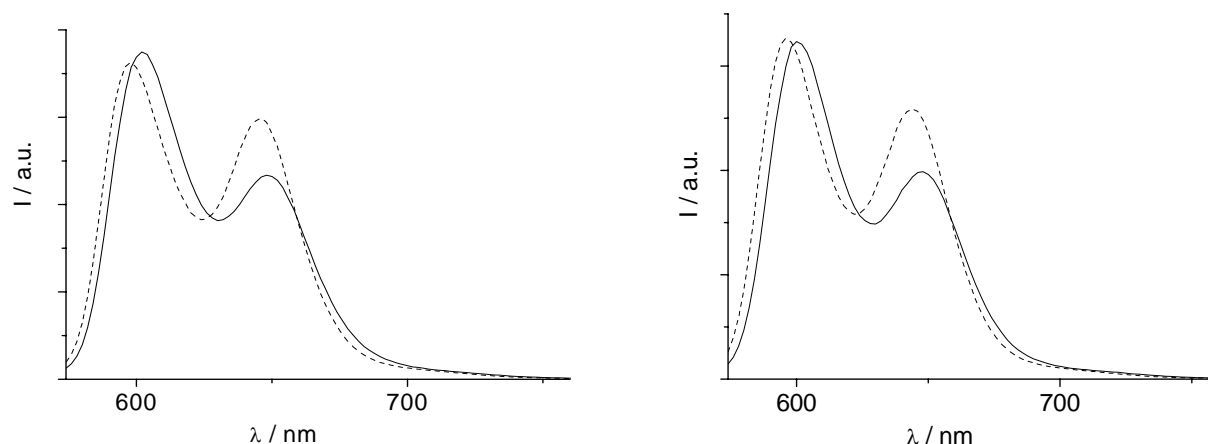


Figure 8S. Uncorrected emission spectra of optically matched solutions of **1a** (solid) and **1b** (dash) in toluene (left) and dichloromethane (right).

Thermodynamic and spectroscopic characterization of model complex **1b₂·3₃** in DCM

The assembly **1b₂·3₃** was prepared in DCM according to the thermodynamic characterization reported below. The concentrations used were 1.1×10^{-6} M for **1b** and 3.18×10^{-4} M for **3**. In these conditions the formation of the **1b₂·3₃** cage is complete: 5×10^{-7} M.

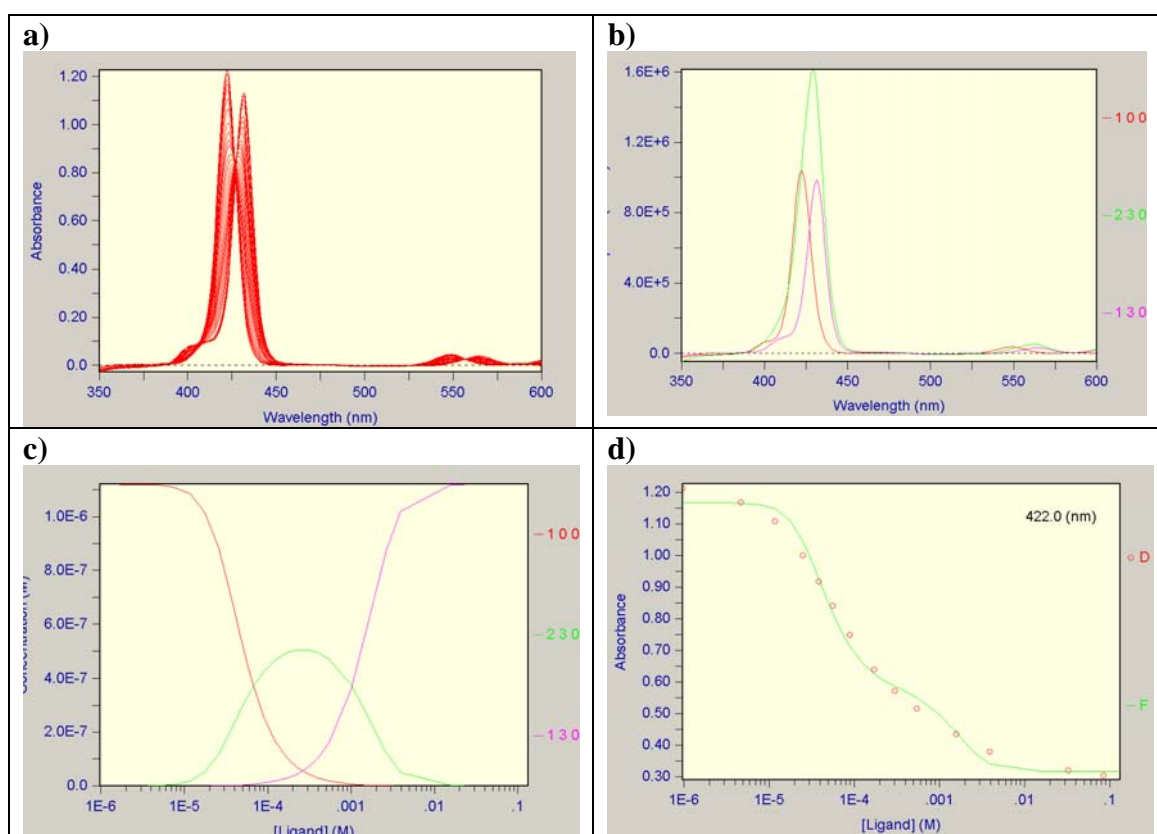


Figure 9S. a) UV-vis titration data of **1b** with **3** in DCM showing the shift of the Soret and Q bands. [**1b**] = 1.1×10^{-6} M. [**2**] = $0 - 13 \times 10^{-2}$ M. b) Calculated UV-vis spectra for the three colored species in equilibrium **1b** (red), **1b₂·3₃** (green) and **3** (pink). c) Simulated concentration profile for the titration of the Zn-trisporphyrin **1b** at 1×10^{-6} M constant concentration with **3** in DCM: **1b** (red), **1b₂·3₃** (green) and **1b·3₃** (pink). d) UV-vis titration data (422 nm) for the binding of **1b** with **3** fitted to the calculated binding curve of a binding model considering free **1b**, **1b₂·3₃** double decker complex and open **1b·3₃** complex.

Table 3S . Calculated stability constants (K) in DCM for the self-assembled $\mathbf{1b}_2\cdot\mathbf{3}_3$ cage and the $\mathbf{1b}\cdot\mathbf{3}_3$ open complex of $\mathbf{1b}$ with $\mathbf{3}$. The microscopic binding constant for the $\text{N}\cdots\text{Zn}$ interaction (K_m) is also reported

Trisporphyrin	Diamine	$K_{23}[\text{M}^{-4}]$	$K_{13}[\text{M}^{-3}]$	$K_m[\text{M}^{-1}]^a$
1b	3	1×10^{19}	5×10^{10}	2×10^3

^a Calculated considering $K_m = (K_{31}/8)^{1/3}$

Absorption spectra of **1b** and the model ZnTPPP in DCM

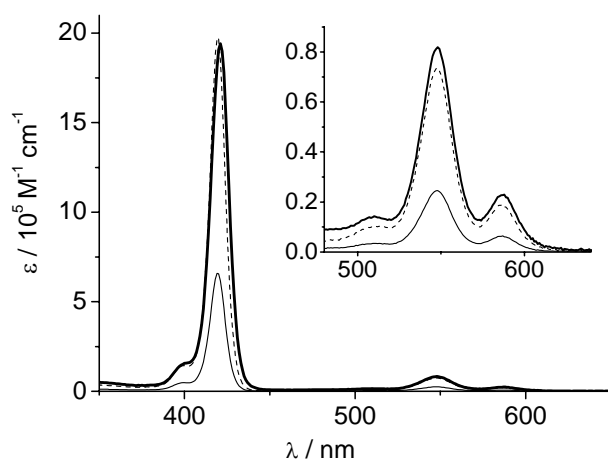


Figure 10S. Absorption spectra of **1b** (thick solid) and the model **ZnTPPP** (thin solid) in dichloromethane. Three times the absorption of **ZnTPPP** is also reported (dash).

Emission spectra of models **1b**, **2**, and $\mathbf{1b}_2\cdot\mathbf{3}_3$ in DCM and TL solutions

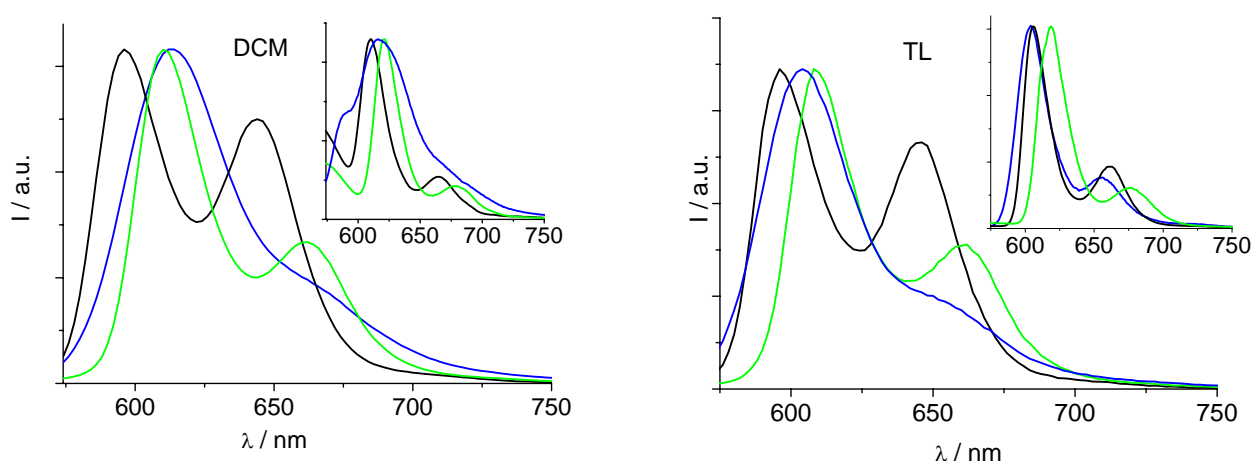


Figure 11S. Normalized uncorrected emission spectra at right angle set up of solutions of **1b** (black), $\mathbf{1b}_2\cdot\mathbf{3}_3$ (green) and **2** (blue) at room temperature. In the inset are reported the luminescence spectra in glass at 77 K.